Journal of Power Sources 207 (2012) 120–126

Contents lists available at SciVerse ScienceDirect

Journal of Power Sources

journal homepage: www.elsevier.com/locate/jpowsour

Hydrogen generation by hydrolysis of alkaline $NaBH_4$ solution on Co–Mo–Pd–B amorphous catalyst with efficient catalytic properties

Yanchun Zhao[a,*], Zhen Ning[a], Jianniao Tian[a], Huaiwen Wang[b], Xiaoyu Liang[a], Sulian Nie[a], Yi Yu[a], Xiaoxiao Li[a]

[a] Key Laboratory for the Chemistry and Molecular Engineering of Medicinal Resources (Ministry of Education of China), College of Chemistry and Chemical Engineering, Guangxi Normal University, Guilin 541004, PR China
[b] Laboratory for Molecular Biology and Cytometry Research, The University of Oklahoma Health Sciences Center, Oklahoma City, OK 73104, USA

ARTICLE INFO

Article history:
Received 3 December 2011
Received in revised form 17 January 2012
Accepted 18 January 2012
Available online 8 February 2012

Keywords:
Co–Mo–Pd–B catalyst
Hydrogen generation
Sodium borohydride
Fuel cells

ABSTRACT

Mo-modified Co–Pd–B (Co–Mo–Pd–B) and Pd-modified Co–B (Co–Pd–B) catalyst powders are synthesized by chemical reduction of cobalt and molybdenum salt at ambient conditions. The resulting catalyst powders are characterized by scanning electron microscopy (SEM), X-ray powder diffraction (XRD), X-photoelectron spectroscopy (XPS) and BET surface area measurement. The study on the catalytic efficiency of amorphous Co–Mo–Pd–B catalyst powders is performed in hydrogen generation by hydrolysis of alkaline sodium borohydride ($NaBH_4$). The Co–Mo–Pd–B powders show the highest hydrogen generation rate as compared to Co–B, Co–Mo–B, and Co–Pd–B catalyst powders. Kinetic studies on the hydrolysis reaction of $NaBH_4$ with Co–Mo–Pd–B catalyst reveal that the concentrations of both $NaBH_4$ and NaOH have essentially no evident effects on hydrogen generation rate. The promoting effect of Mo in Co–Mo–Pd–B catalyst results in lower activation energy for hydrogen production, which is 36.36 kJ mol^{-1} compared to 64.87 kJ mol^{-1} obtained with pure Co–B powder.

1. Introduction

It is known that hydrogen is an almost zero discharge kind of clean energy. The chemical energy of hydrogen can be directly changed into electric energy, producing only water as a byproduct, when hydrogen gas is used in proton exchange membrane fuel cells (PEMFC) or other kind of energy equipment [1,2]. Therefore, the development of an effective and safe medium for hydrogen storage and generation is in favor of the commercialization of PEMFC or other fuel cell-based portable devices. In recent years, chemical hydride ($NaBH_4$, $LiBH_4$, NaH, KBH_4, etc.), as one of the most prospective hydrogen storage materials at room temperature, receives the most extensive attention, especially sodium borohydride ($NaBH_4$) [3]. With hydrogen storage capability of 10.8 wt.%, $NaBH_4$ is non-flammable, non-toxic in nature and stable in alkaline solution. Its hydrolysis reaction may be represented by the following equation [4]:

$$NaBH_4 + 2H_2O \xrightarrow{\text{catalyst}} NaBO_2 + 4H_2 + \text{Heat}\,(217\,\text{kJ}) \quad (1)$$

In past few years, many researchers devoted themselves to researches of catalyst for hydrolysis of sodium borohydride. They found that hydrolysis reaction rate of $NaBH_4$ alkaline solution can be effectively increased by using solid state catalysts such as precious metals [5–7]. Noble catalysts such as Pt, Pd, and PtRu supported on C [5,8], $LiCoO_2$ [7,9], Ru supported on graphite [10], Rh/Al_2O_3 and Rh/TiO_2 [11] have been utilized in order to improve the hydrogen production rate. Unfortunately, these precious catalysts have no viability for industrial application considering their cost and scarcity. Cheaper candidates in form of transition metals such as cobalt boride (Co–B) catalyst [12–14] have been used to accelerate the hydrolysis reaction of $NaBH_4$. Co–B catalyst material can be easily synthesized by simple chemical processes [13]. However, the exothermic nature of this reaction causes Co–B particles to agglomerate due to a high surface energy involved [15]. This agglomeration of particles decreases the effective surface area of the catalyst powder thus limiting the catalytic activity. To minimize agglomeration, Co–B was deposited on different support materials with specific surface features such as Ni foam [16], carbon nanotubes [17], the modified activated carbon [18], and attapulgite clay [19]. Mesoporous and hollow sphere Co–B catalysts were also synthesized by Tong et al. [20] and Ma et al. [21], respectively. The final surface area of these catalyst powders is much higher than that of the "normal" Co–B catalyst. On the other hand, Patel et al. used another efficient route to avoid agglomeration of Co–B particles by introducing atomic barrier with transition metals including Cr, Mo, and W [15,22]. Previous reports showed that transition metal-doped Co–B alloy catalysts in form of Co–Cr–B [15], Co–Ni–B [23],

* Corresponding author. Tel.: +86 773 5846279; fax: +86 773 2120958.
E-mail address: yanchunzh@yahoo.cn (Y. Zhao).

0378-7753/$ – see front matter © 2012 Elsevier B.V. All rights reserved.
doi:10.1016/j.jpowsour.2012.01.118

Co–Cu–B [24], Co–Ni–P–B [25] and Co–M–B/Ni foam (M = Mo, W) [26,27] exhibit superior catalytic activity in hydrogen production by hydrolysis of $NaBH_4$. As compared to that of Co–B, a several-fold increment of surface area was found for Co–M–B (M = Ni, Fe, Cu, Cr, Mo, and W), in which these promoter metals were in the form of oxide [15,28]. Consequently, the addition of transition metal greatly improved the performance of Co–B catalyst. In addition, Liang et al. [29] found that Co–B catalyst was more easily supported on nickel foam substrate modified with a small amount of the noble metal Pd. The doping of Pd significantly enhanced the performance and stability of Co–B/Pd for hydrolysis reaction of $NaBH_4$ during the long-term operation.

In this work, the catalytic activity of Co–Pd–B catalyst powders was enhanced tremendously by introducing the noble metal Pd in Co–B, as compared to pure Co–B. In these catalysts only a minimal amount for Pd is used and it greatly improves the catalytic performance of Co–B towards the hydrolysis reaction of $NaBH_4$, therefore the cost for this Co–Pd–B catalyst is greatly reduced, compared to those noble-metal-only catalysts such as Ru/IR-120 [30], Ru (0) nanoclusters [6], Pt–Pd [31], and Rh [11]. Further, the Co–Pd–B catalyst is modified by addition of the transition metal molybdenum (Mo) and the hydrogen generation rate on this Mo-modified Co–Pd–B catalyst, Co–Mo–Pd–B, is much higher than that of Co–Pd–B catalyst by itself. Hence, through the combination of the superiority of the noble metal Pd with the less expensive transition metal Mo to the Co–B alloy catalysts, the purpose of reducing cost and meanwhile significantly improving efficiency of the catalysts was achieved. The Mo-modified Co–Pd–B catalyst powders (Co–Mo–Pd–B) was synthesized by chemical reduction method, and the particle size was controlled by adding surfactant at the same time. The hydrogen production process through catalytic hydrolysis of $NaBH_4$ was investigated in the presence of the Co–Mo–Pd–B catalyst. The Co–Mo–Pd–B powders exhibit superior catalytic activity, as compared to pure Co–B and Co–Pd–B powders, owing to their high surface area and facilitation of doped Pd and Mo. An enhanced catalytic activity of the prepared catalyst for hydrolysis of alkaline $NaBH_4$ solution further suggested the promising applications in PEMFC.

2. Experimental

The Co–Mo–Pd–B powder catalyst was synthesized by chemical reduction method. Sodium borohydride ($NaBH_4$, 300 mg in 10 mL water), as a reducing agent, was added into an aqueous solution containing cobalt salt ($CoCl_2{\cdot}6H_2O$, 0.2038 g), molybdenum salt (Na_2MoO_4, 25 mM) and trisodium citrate (20 mM) under vigorous stirring. An excess amount of borohydride was used so that the reaction was absolutely complete, and a black turbid liquid was observed. Then H_2PdCl_4 (10 mM) was added into the black solution under vigorous stirring and the solution was continuously stirred for two hours. An extra amount of borohydride (50 mg in 5 mL water) was added and the mixture was continuously stirred for two hours again. The black powder was separated from the solution by filtration and then washed extensively with distilled water and ethanol before being dried overnight in oven at 323 K. The molar ratio of Mo/(Mo + Co) (atom %) (χ_{Mo}) was adjusted in the final Co–Mo–Pd–B catalyst powder by varying the molar concentration of Na_2MoO_4 in the aqueous solution. To make experiments comparable, the Co–B and Co–Pd–B powders were prepared with the same procedure as the Co–Mo–Pd–B catalyst in the absence of molybdenum salt, respectively.

The surface morphology and the composition of all the catalyst powders were studied by SEM (FEI Quanta 200 FEG, Holland) equipped with energy-dispersive spectroscopy analysis (EDS). Structural characterization of the catalyst powders was performed using X-ray powder diffraction (XRD) on a Rigaku D/max 2500 v/pc diffractometer (Japan) with filtered Cu Ka radiation. Surface electronic states and the related atomic composition of the catalysts were established using X-ray photoelectron spectroscopy (XPS, JPS-9010TR) with Mg Ka radiation. The BET surface area of the powder catalysts was determined by nitrogen absorption at 77 K (Micromeritics ASAP 2010) after degassing.

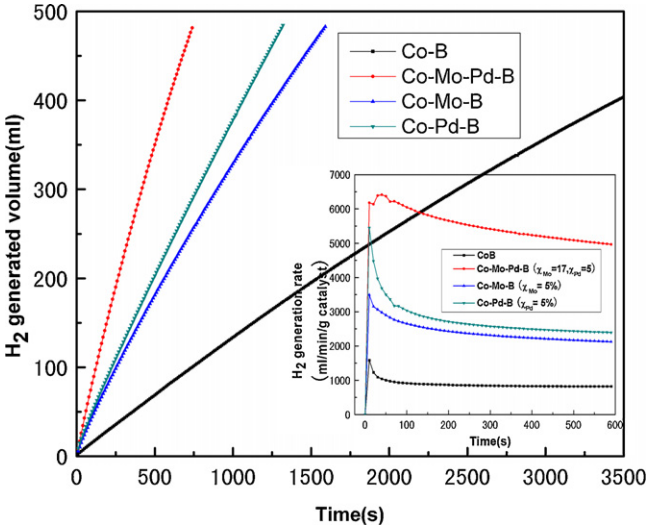

Fig. 1. Hydrogen generated volume as a function of reaction time obtained by hydrolysis of alkaline $NaBH_4$ (150 mM) with Co–B, Co–Mo–B (χ_{Mo} = 5%), Co–Pd–B (χ_{Pd} = 5%) and Co–Mo–Pd–B (χ_{Mo} = 17%, χ_{Pd} = 5%) catalyst powders. Inset shows the real-time H_2 generation rate of different catalysts treated at the same condition.

An alkaline-stabilized solution of sodium borohydride (0.150 M) was prepared by the addition of NaOH (5 wt.%) for catalytic activity measurements. A detailed description of the measurement apparatus was reported in Ref. [17], and a gas volumetric method used for the measurement of the generated hydrogen quantity is similar to that reported in Ref. [17]. By weight of displaced water and gas pressure, the amount of hydrogen produced is quantified. In all measurement cycles, the catalyst was settled on the appropriate device, in which the reaction chamber was sealed. A certain amount of catalyst powder (10 mg) was added to 50 mL of the above alkaline $NaBH_4$ solution at 298 K under continuous stirring. Each measurement was repeated at least 3 times.

Different experimental parameters such as solution temperature, starting concentration of NaOH and $NaBH_4$ were varied for kinetic study on $NaBH_4$ hydrolysis using Co–Mo–Pd–B catalysts. The activation energy involved in the catalytic hydrolysis reaction was determined by measuring H_2 generation rate at different solution temperatures. Furthermore, the corresponding activity of the solution was investigated by varying concentrations of NaOH (1–7 wt.%) and $NaBH_4$ (0.050–0.200 M), in which one parameter was changed while other parameter was kept constant. The specific hydrogen generation rate (mL min^{-1} g^{-1} catalyst) was used to compare the activities of the catalysts.

3. Results and discussion

Hydrogen generated volume was measured as a function of time during the hydrolysis of alkaline $NaBH_4$ (0.150 M) solution in the presence of different catalyst powders at 298 K (Fig. 1). The Co–Mo–Pd–B catalyst shows the highest catalytic activity for hydrogen generation as compared to that of Co–B, Co–Mo–B, and Co–Pd–B catalyst, under the same amount (10 mg) of the catalyst. A numerical procedure, described elsewhere [32], was utilized to obtain the maximum value of the hydrogen generation rate (R_{max}) for all the catalyst powders. The R_{max} obtained with Co–Mo–Pd–B

Table 1
Comparison of max. hydrogen generation (HG) rates on various catalysts.

Catalyst	Initial solution temperature for max. HG (°C)	$NaBH_4$ concentration	NaOH concentration	Maximum HG rate ($mL\,min^{-1}\,g^{-1}$ catalyst)	Reference
Co–B/C	25	0.2 M	2 M	~2073	[45]
Co–Cu–B	20	7 wt.%	7 wt.%	~2120	[24]
Co–Cr–B	25	0.025 M	0.1 M	~3400	[15]
Co–Mo–B	25	0.025 M	0.1 M	~2875	[22]
Co–W–B	25	0.025 M	0.1 M	~2570	[22]
Co–B	25	0.025 M	0.1 M	~850	[22]
Co–Ni–B	25	0.025 M	0.1 M	~1175	[23]
Co–B/MWCNTs	30	20 wt.%	3 wt.%	~5100	[17]
Ru/C (graphite)	30	10 wt.%	5 wt.%	~32,300	[10]
PtRu–$LiCoO_2$	25	5 wt.%	5 wt.%	~2400	[7]
Ni–Ru/50WX8	35	10 wt.%	5 wt.%	~400	[46]
Co–B/Pd	30	20 wt.%	4 wt.%	~2875	[29]
Co–Pd–B	25	0.150 M	5 wt.%	~2920	This work
Co–Mo–Pd–B	25	0.150 M	5 wt.%	~6023	This work

(χ_{Mo} = 17%, χ_{Pd} = 5%) is ~6023 $mL\,min^{-1}\,g^{-1}$, which is twice as much as with Co–Pd–B (~2920 $mL\,min^{-1}\,g^{-1}$) and seven folds higher than that with pure Co–B (~850 $mL\,min^{-1}\,g^{-1}$). The result clearly indicates that addition of Mo to the Co–Pd–B catalyst significantly enhance the catalytic activity. The comparison of R_{max} of the Co–Mo–Pd–B catalyst as well as those of other catalysts was given in Table 1.

Fig. 2 presents the effect of Mo concentration on catalytic activity which were studied by varying the percentage of Mo/(Mo + Co) molar ratio (χ_{Mo}) from 1% to 25% in the Co–Mo–Pd–B (χ_{Pd} = 5%) powder catalyst. The inset of Fig. 2 shows the plot of R_{max} as a function of χ_{Mo}. The promoting effect of Mo on catalytic activity is so evident that even a small amount of doping (χ_{Mo} = ~1%) is able to double the activity of Co–Pd–B catalyst. The H_2 generation rate increases with Mo concentration and reaches the maximum when χ_{Mo} is about 17%. With further increase of χ_{Mo}, the activity of the powder decreases.

The BET surface areas of the Co–Pd–B and Co–Mo–Pd–B catalysts, calculated by the Brunauer–Emmett–Teller (BET) equation, were 20.3 and 34.7 $m^2\,g^{-1}$, respectively. From BET values, it can be seen that the addition of the Mo-promoter enhances the BET surface area by almost 2 times, due to the limited particle agglomeration process in Co–Mo–Pd–B as compared to Co–Pd–B (see Fig. 3) [15,22]. The bigger BET value shows that the Co–Mo–Pd–B catalyst owns a larger surface area than Co–Pd–B catalyst. A larger BET surface area is beneficial for enhancing the active surface area of Co–Mo–Pd–B. This agrees well with the result of Patel et al. [15,22,24]. The increase of the active surface area of catalysts is helpful to improve the catalytic activity of Co–Mo–Pd–B toward hydrolysis of alkaline $NaBH_4$ solution [15,24]. The consequence can be confirmed once again in Fig. 3 as follow. However, large Mo doping is harmful to the catalyst's activity because Mo would cover most of the active Co sites [15]. Thus a well-defined χ_{Mo} value is required (χ_{Mo} = 17%, χ_{Pd} = 5% as shown in Fig. 2) to attain the best conditions for the catalytic activity of Co–Mo–Pd–B catalyst in hydrolysis reaction of alkaline $NaBH_4$ solution.

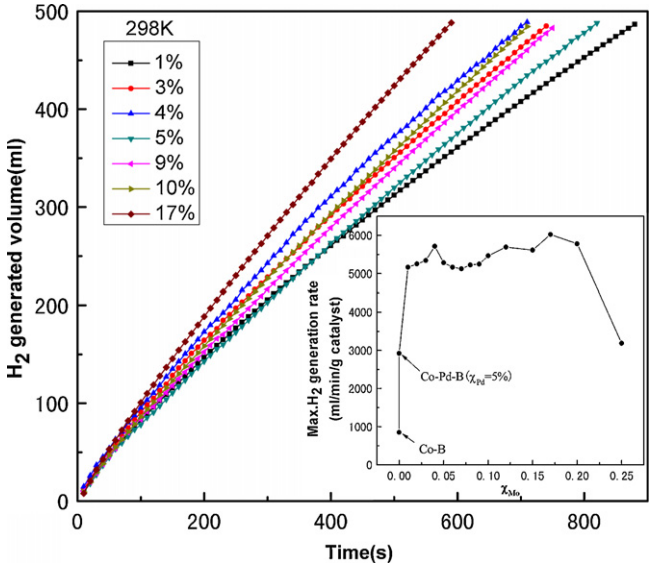

Fig. 2. Hydrogen generated volume as a function of reaction time obtained by hydrolysis of alkaline $NaBH_4$ (0.150 M) with Co–Mo–Pd–B (χ_{Pd} = 5%) catalyst with different Mo/(Mo + Co) molar ratios ranging from 1% to 25%. Inset shows the maximum H_2 generation rate (R_{max}) obtained with Co–Mo–Pd–B catalyst as a function of χ_{Mo}.

Fig. 3 presents the SEM images of Co–Pd–B (χ_{Pd} = 5%) and Co–Mo–Pd–B (χ_{Mo} = 17%, χ_{Pd} = 5%) powders. The SEM images of both catalysts show similar particle-like morphology with size of dozens of nanometers. More agglomeration of the small particles can be seen in the SEM image of Co–Pd–B catalyst. The particle size distribution in Co–Mo–Pd–B catalyst is opposite to that of Co–Pd–B catalyst. The catalyst doped with Mo consists of much more uniform particle with less amount of agglomeration and such morphology is helpful to enhance the active surface area of catalysts [15]. This is the result of the introduction of Mo as an atomic barrier [15]. The higher active surface area of the catalysts is conducive to improved catalytic performance.

As can be seen from the XRD diffractogram (Fig. 4), the samples present a very low level of crystallinity [15], because there is no distinct sharp peak observed. XRD patterns of four catalyst powders show a wide and diffuse peak centered at about 2θ = 45°, which is attributed to the amorphous state of cobalt-metalloid alloy [15,19]. The assignment of the peaks leads to the identification of Co_2B phase, Co, CoO, Co_3O_4 and the possible presence of minor phases as cobalt borate and/or hydroxide [33]. This phenomenon may be assumed to be surface Co combined with oxygen of atmosphere during the process of catalyst preparation [33]. Moreover, the broad peak at around 2θ = 37° attributed to the presence of MoO_2 is observed for Co–Mo–Pd–B catalyst powder, as is resembled to that reported for XRD patterns of Mo in the literature [34]. The diffraction peaks of the Pd and PdO phases were also shown at 2-theta angles of around 43°, 52°, 68°, 75° and 82° in Co–Pd–B and Co–Mo–Pd–B catalysts [35].

Fig. 5 reports the XPS spectra of Co_{2p} (a), B_{1s} (b), Mo_{3d} (c), and Pd_{3d} (d) electronic levels in fresh Co–B, Co–Mo–B (χ_{Mo} = 5%), Co–Pd–B (χ_{Pd} = 5%) and Co–Mo–Pd–B (χ_{Mo} = 17%, χ_{Pd} = 5%) catalyst powders. The electronic state and surface interaction between atoms in compounds was obtained in XPS spectra to understand

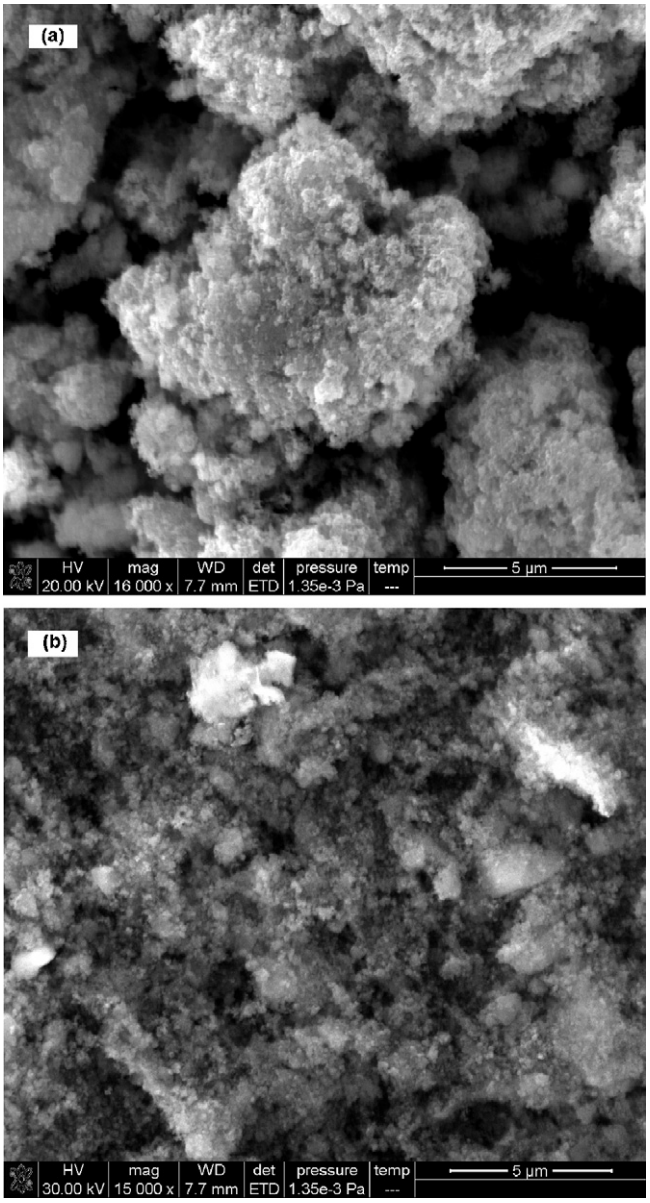

Fig. 3. SEM micrographs of Co–Pd–B (χ_{Pd} = 5%) (a) and Co–Mo–Pd–B (χ_{Mo} = 17%, χ_{Pd} = 5%) (b) catalyst powders.

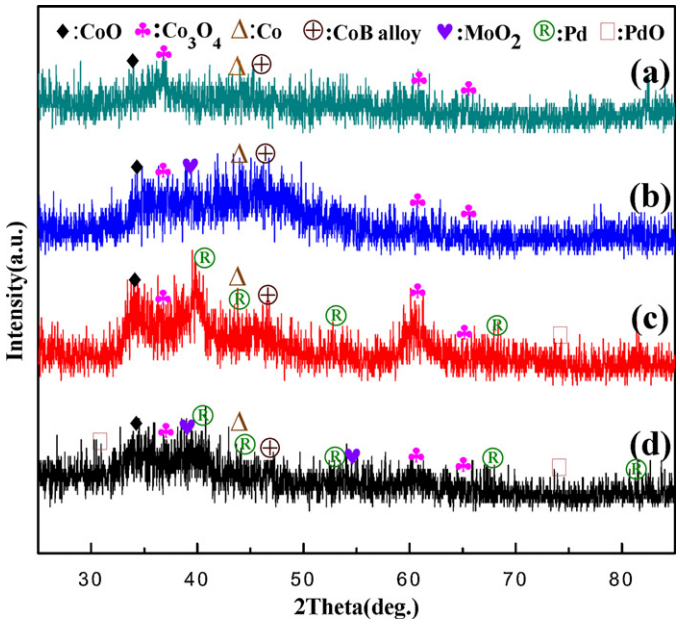

Fig. 4. XRD pattern of (a) Co–B, (b) Co–Mo–B (χ_{Mo} = 5%), (c) Co–Pd–B (χ_{Pd} = 5%) and (d) Co–Mo–Pd–B (χ_{Mo} = 17%, χ_{Pd} = 5%) catalyst powders.

the promoting effect of Mo on the catalytic activity of Co–Pd–B [15]. For all catalysts, it can be seen that two peaks corresponding to the $Co_{2p3/2}$ and $Co_{2p1/2}$ are centered at approximately 781.6 and 797.6 eV, respectively, which meet the values of the metallic state of Co [36–38] and thus indicate that Co element exists in both elemental and oxidized states [15]. The 2^+ state related to the peak of the oxidized cobalt is attributed to $Co(OH)_2$ [15,23] which could have possibly been formed during the catalyst preparation. There are different extents of positive shift in the Co peaks of these compound catalysts compared to the standard binding energy (BE) of metallic Co (778.4 and 781.6 eV). In general, a larger BE indicates the presence of more oxidized states [39,40]. The XPS peaks are also observed about at BE values of 191.6 eV, which correspond to oxidized B_{1s} levels in Co–B, Co–Mo–B, Co–Pd–B, and Co–Mo–Pd–B, similar to that reported for B_{1s} levels in the literature [23]. There is an evident positive shift of 4.4 eV when comparing the BE of pure boron (187.1 eV) [15] to that of boron in the catalyst. This shift demonstrates electron transfer from alloying B to vacant d-orbital of metallic Co [15,28]. As for Mo, the Mo_{3d} spectrum for the Co–Mo–Pd–B catalyst exhibits two peaks (232.0 and 234.2 eV), which were attributed to $Mo_{3d5/2}$ and $Mo_{3d3/2}$ peaks of Mo^{4+}, Mo^{6+} species [41,42] and thus ascribed to MoO_2 and MoO_3 [22,41,42], respectively. This result agrees with the XRD pattern, which describes that all the Mo particles are at oxidized state. The molybdenum oxide serves as a kind of barrier among the Co–Pd–B nanoparticles resulting in smaller particle size with uniform distribution, thus averting agglomeration due to their high surface energy [15]. As a result, the effective surface area increases significantly in the Co–Mo–Pd–B catalyst. The curve shape of Fig. 5(d) overlaps with peaks of 336.2 eV for the 3d 5/2 BE of Pd, and 341.6 eV for the 3d3/2 BE of Pd, which indicates that the valence state of palladium is oxidation state according to the BE of Pd^0 at 335.1 eV [43].

Fig. 6 presents the H_2 generated volume as a function of time at different solution temperatures using alkaline $NaBH_4$ (0.150 M) solution. The linear relation between temperature and hydrogen generation rate can generally be expressed with the Arrhenius equation [24]:

$$\ln\ k = \ln\ k_0 - E_a \cdot \frac{1}{RT} \quad (2)$$

According to Arrhenius equation, the Arrhenius plot of the hydrogen production rate (inset of Fig. 6) gives an activation energy value of the catalytic hydrolysis process of about 36.36 kJ mol^{-1}, which is lower than that obtained with Co–B powder (64.87 kJ mol^{-1}) [12], Co–Cu–B (49.6 kJ mol^{-1}) [24], Co–B hollow spheres (45.5 kJ mol^{-1}) [21], Co–P (48.1 kJ mol^{-1}) [44], Co–B/C (57.8 kJ mol^{-1}) [45], Co–B/MWCNTs (40.40 kJ mol^{-1}) [17], and the Co–Mo–B/nickel foam catalyst (44.3 kJ mol^{-1}) [26]. This value is also lower than that obtained with $Pt/LiCoO_2$ (70.4 kJ mol^{-1}) and $Ru/LiCoO_2$ (68.5 kJ mol^{-1}) [9], Ni–Ru/50WX8 catalyst (52.73 kJ mol^{-1}) [46], Ru/G (61.10 kJ mol^{-1}) [10], and the Ru catalyst (47 kJ mol^{-1}) [4]. The activation energy value obtained in the present case is comparable to that obtained with Co–Ni–B (34 kJ mol^{-1}) [23], Co–Cr–B (37 kJ mol^{-1}) [15], intrazeolite Co (0) nanoclusters (36 kJ mol^{-1}) [47], Co–B/Ni foam (33 kJ mol^{-1}) [16], Ru (0) nanoclusters (28.51 kJ mol^{-1}) [6], and the Pd/C powder (28 kJ mol^{-1}) [8]. The favorable activation energy value obtained in the present work, which lead to an improvement in catalytic

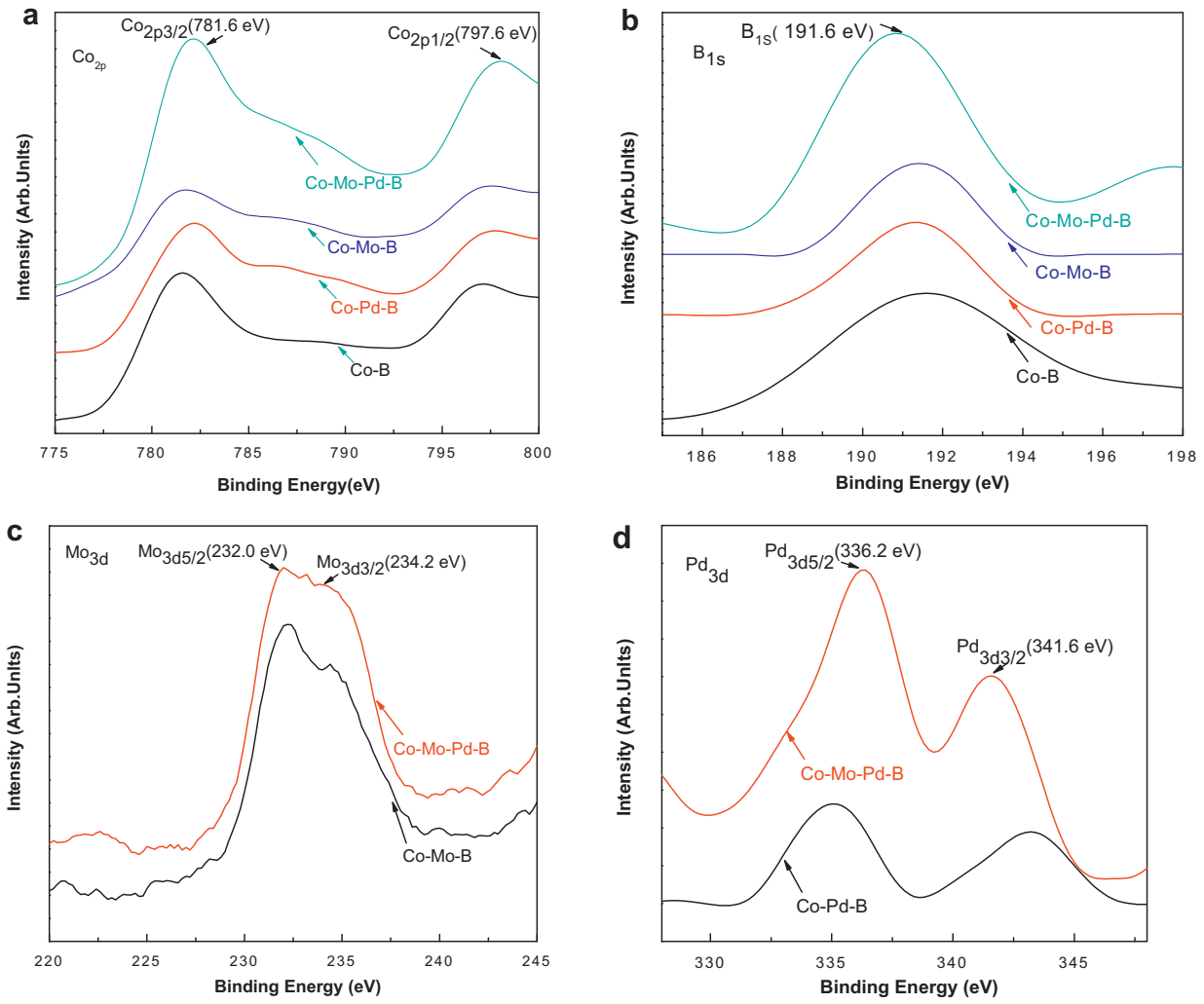

Fig. 5. X-ray photoelectron spectra of Co_{2p3} (a), B_{1s} (b), Mo_{3d} (c), and Pd_{3d} (d) levels for Co–B, Co–Mo–B (χ_{Mo} = 5%), Co–Pd–B (χ_{Pd} = 5%) and Co–Mo–Pd–B (χ_{Mo} = 17%, χ_{Pd} = 5%) catalyst powders.

hydrolysis performance, is attributed to both the high surface area and the synergetic effects of Co, Mo, and B in the Co–Mo–Pd–B catalyst [15,25].

Fig. 7 shows the plot of hydrogen generated volume as a function of time, obtained from hydrolysis of alkaline $NaBH_4$ solution by using five different $NaBH_4$ concentrations, namely: 0.05, 0.075, 0.10, 0.150 and 0.200 M in the starting solution. The concentration of NaOH and the Co–Mo–Pd–B catalyst (χ_{Mo} = 17%, χ_{Pd} = 5%) was kept constant at 5 wt.% and 10 mg, during the hydrolysis reaction, respectively. The result clearly indicates that there is a slight increase in the hydrogen generation rate with the increase of the $NaBH_4$ concentration. However, as shown in the inset of Fig. 7, the logarithmic dependence of R_{max} from $NaBH_4$ concentration can be fitted with a straight line with a slope of 0.18. The near-zero value of the slope indicates the zero order kinetics of the reaction with respect to the $NaBH_4$ concentration for the Co–Mo–Pd–B catalyst, thus confirming our previous findings. Similar zero order kinetics was proposed by Özkar and Zahmakıran [6] (Ru (0) nanoclusters), Amendola et al. [4] (Ru catalyst), and Fernandes et al. [15] (Co–Cr–B) for reactions with high $NaBH_4$ concentration.

According to the hydrolysis reaction mechanism proposed in Ref. [8], the initial reaction for H_2 generated from the metal-catalyzed hydrolysis of $NaBH_4$ occurs between BH_4^- ions and metal sites, which implies that the reaction rate is proportional to the number of available metal sites for the absorption of BH_4^- ions

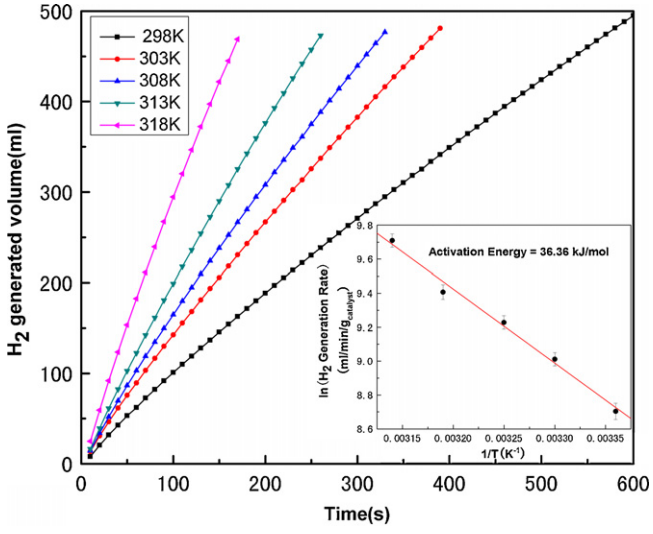

Fig. 6. Hydrogen generated volume as a function of reaction time by hydrolysis of alkaline $NaBH_4$ (0.150 M) solution with Co–Mo–Pd–B (χ_{Mo} = 17%, χ_{Pd} = 5%) catalyst, measured at five different solution temperatures. Inset shows the Arrhenius plot of the H_2 generation rates.

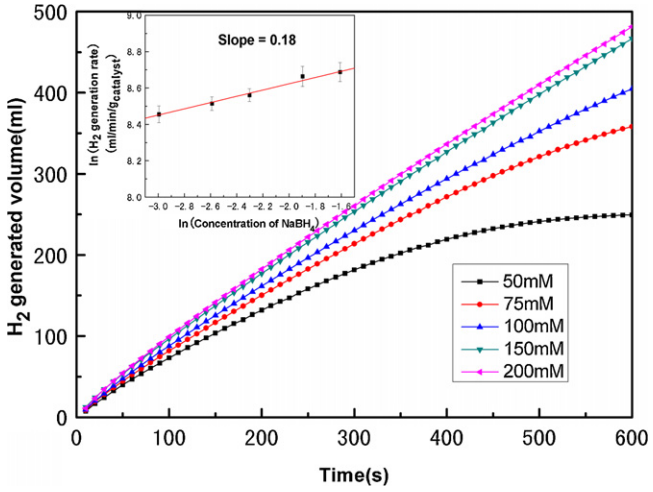

Fig. 7. Hydrogen generated volume as a function of reaction time with Co–Mo–Pd–B (χ_{Mo} = 17%, χ_{Pd} = 5%) catalyst obtained by hydrolysis of alkaline $NaBH_4$ solution with five different concentrations of $NaBH_4$ ranging from 0.050 to 0.200 M. Inset shows the plot of ln(H_2 generation rate) vs. ln(concentration of $NaBH_4$).

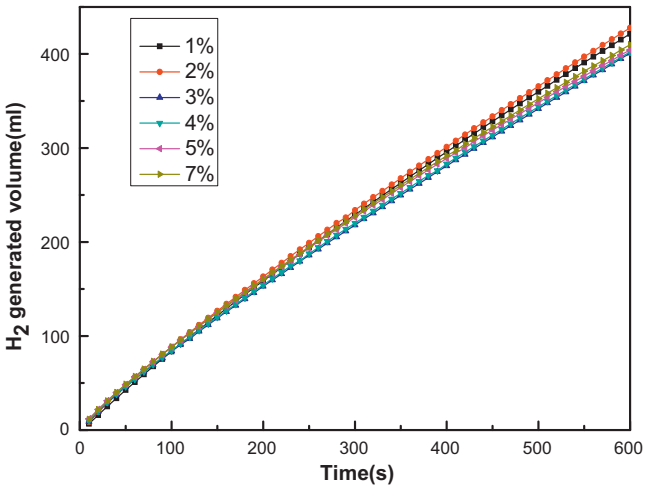

Fig. 9. Hydrogen generated volume as a function of reaction time with Co–Mo–Pd–B (χ_{Mo} = 17%, χ_{Pd} = 3%) catalyst obtained by hydrolysis of alkaline $NaBH_4$ (0.150 M) solution with six different concentrations of NaOH ranging from 1 to 7 wt.%.

in the solution. Fernandes et al. [15] thought that Cr^{3+} species in surface of the Co–Cr–B catalyst powder could act as Lewis acid sites, which were readily available for the absorption of Lewis base such as OH^- ions during the hydrolysis reaction of alkaline $NaBH_4$. Similar promoting effect by Cr metal was reported by Fang et al. [28] and Kukula et al. [48] using Ni–Cr–B and Co–Cr–B catalyst for hydrogenation of 2-ethylanthraquinone and nitriles, respectively. In order to demonstrate that Mo^{4+} species in Co–Mo–Pd–B catalyst have similar promoting effect, two types of hydride solution (0.15 M) were prepared: (1) $NaBH_4$ solution stabilized with NaOH (5 wt.%) (designated as solution A) and (2) $NaBH_4$ solution without NaOH (designated as solution B). Fig. 8 reports hydrogen generation rate obtained by hydrolysis of solutions A and B using Co–Mo–Pd–B (χ_{Mo} = 17%, χ_{Pd} = 5%) and Co–B catalyst powders. Anterior researches [15] have shown that no significant change in H_2 generation rate was observed through the hydrolysis process of alkaline and non-alkaline $NaBH_4$ in the presence of Co–B catalyst powder. However, the H_2 generation rate obtained by hydrolysis of $NaBH_4$ in the presence of Co–Mo–Pd–B for solution A was much higher than that of solution B, as show in Fig. 8. The R_{max} value measured with the Co–Mo–Pd–B catalyst by hydrolysis of solutions A and B is 7 and 4 times higher than that obtained with the Co–B catalyst, respectively. This result proves that during the hydrolysis reaction in alkaline condition, Mo^{4+} species acting as Lewis acid sites are able to absorb the OH^- group and catalyze the reaction between OH^- and boron species (BH_3^-, $BH_2(OH)^-$, and $BH(OH)_2^-$). This promoting effect contributes to the overall catalytic reaction.

Fig. 9 represents the effect of the pH of the reaction solution on hydrolysis reaction rate of $NaBH_4$. The process was performed by measuring the volume of the generated H_2 from hydrolysis of alkaline $NaBH_4$ by using seven different NaOH concentrations from 1 to 7 wt.% in the starting solution. The result shows that there is only a very slight change in the hydrogen generation rate (R_{max}) with the increase of NaOH content, which indicates the zero order reaction with respect to NaOH concentration. The result also implies

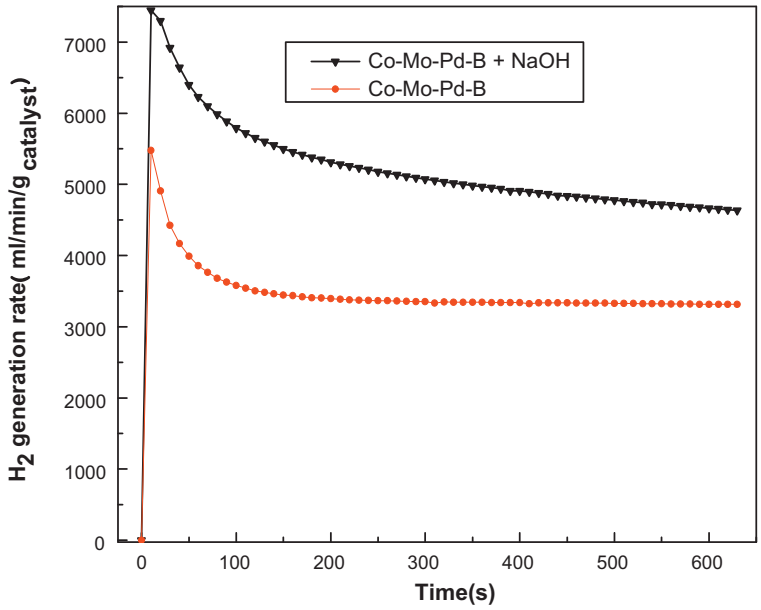

Fig. 8. Hydrogen generated rate as a function of reaction time obtained by hydrolysis of alkaline and non-alkaline $NaBH_4$ solution using Co–Mo–Pd–B (χ_{Mo} = 17%, χ_{Pd} = 5%) catalyst powders.

that the Co–Mo–Pd–B catalyst is promising for applications in the industrial production, because the hydrolysis reaction process with the Co–Mo–Pd–B catalyst does not require strict controlling for the concentration of NaOH.

4. Conclusions

In summary, the catalytic activity of Co–Mo–Pd–B powder on hydrogen production by hydrolysis of alkaline $NaBH_4$ solution was studied. The rate of hydrogen production depends on the $\chi_{Mo} = Mo/(Mo + Co)$ parameter and the maximum value of the rate is observed when $\chi_{Mo} = 17\%$. The catalytic activity is twice as much as Co–Pd–B catalyst at a χ_{Mo} of 17%, and about 7 times higher than that of the pure Co–B catalyst. Characterization results show that this superior catalytic activity is related to the formation of molybdenum oxide on the catalyst surface, which avoids agglomeration of the Co–Pd–B particles and thus increases the final active surface area of the Co–Mo–Pd–B powder catalyst. The promoting effect of Mo in the Co–Mo–Pd–B catalyst results in lower activation energy for hydrogen production, which is 36.36 kJ mol^{-1} compared to 64.87 kJ mol^{-1} of pure Co–B. The favorable activation energy value obtained in the present work is attributed to both the high surface areas and the synergetic effects of Co, Mo, and B in Co–Mo–Pd–B catalyst.

Acknowledgments

This work has been supported by the National Natural Science Foundation of China (No. 21163002, 21165004), Guangxi Natural Science Foundation of China (2010GXNSFF013001, 0728043), the project of Key Laboratory for the Chemistry and Molecular Engineering of Medicinal Resources (Guangxi Normal University), Ministry of Education of China (CMEMR2011-14) and Innovation Plan in Graduate Education of Guangxi Province (2011106020703M48).

References

[1] S.C. Amendola, S.L. Sharp-Goldman, M.S. Janjua, N.C. Spencer, M.T. Kelly, P.J. Petillo, M. Binder, Int. J. Hydrogen Energy 25 (2000) 969–975.
[2] A.M.F.R. Pinto, M.J.F. Ferreira, V.R. Fernandes, C.M. Rangel, Catal. Today 170 (2011) 40–49.
[3] Y. Liang, P. Wang, H.-B. Dai, J. Alloys Compd. 491 (2010) 359–365.
[4] S.C. Amendola, S.L. Sharp-Goldman, M.S. Janjua, M.T. Kelly, P.J. Petillo, M. Binder, J. Power Sources 85 (2000) 186–189.
[5] D. Xu, H. Zhang, W. Ye, Catal. Commun. 8 (2007) 1767–1771.
[6] S. Özkar, M. Zahmakıran, J. Alloys Compd. 404–406 (2005) 728–731.
[7] P. Krishnan, T.-H. Yang, W.-Y. Lee, C.-S. Kim, J. Power Sources 143 (2005) 17–23.
[8] N. Patel, B. Patton, C. Zanchetta, R. Fernandes, G. Guella, A. Kale, A. Miotello, Int. J. Hydrogen Energy 33 (2008) 287–292.
[9] Z. Liu, B. Guo, S.H. Chan, E.H. Tang, L. Hong, J. Power Sources 176 (2008) 306–311.
[10] Y. Liang, H.-B. Dai, L.-P. Ma, P. Wang, H.-M. Cheng, Int. J. Hydrogen Energy 35 (2010) 3023–3028.
[11] Y.V. Larichev, O.V. Netskina, O.V. Komova, V.I. Simagina, Int. J. Hydrogen Energy 35 (2010) 6501–6507.
[12] S.U. Jeong, R.K. Kim, E.A. Cho, H.J. Kim, S.W. Nam, I.H. Oh, S.A. Hong, S.H. Kim, J. Power Sources 144 (2005) 129–134.
[13] J. Lee, K.Y. Kong, C.R. Jung, E. Cho, S.P. Yoon, J. Han, T.-G. Lee, S.W. Nam, Catal. Today 120 (2007) 305–310.
[14] N. Patel, G. Guella, A. Kale, A. Miotello, B. Patton, C. Zanchetta, L. Mirenghi, P. Rotolo, Appl. Catal. A: Gen. 323 (2007) 18–24.
[15] R. Fernandes, N. Patel, A. Miotello, Appl. Catal. B: Environ. 92 (2009) 68–74.
[16] H.-B. Dai, Y. Liang, P. Wang, H.-M. Cheng, J. Power Sources 177 (2008) 17–23.
[17] Y. Huang, Y. Wang, R. Zhao, P.K. Shen, Z. Wei, Int. J. Hydrogen Energy 33 (2008) 7110–7115.
[18] D. Xu, P. Dai, Q. Guo, X. Yue, Int. J. Hydrogen Energy 33 (2008) 7371–7377.
[19] H. Tian, Q. Guo, D. Xu, J. Power Sources 195 (2010) 2136–2142.
[20] D.-G. Tong, W. Chu, Y.-Y. Luo, H. Chen, X.-Y. Ji, J. Mol. Catal. A: Chem. 269 (2007) 149–157.
[21] H. Ma, W. Ji, J. Zhao, J. Liang, J. Chen, J. Alloys Compd. 474 (2009) 584–589.
[22] N. Patel, R. Fernandes, A. Miotello, Catal. J. 271 (2010) 315–324.
[23] R. Fernandes, N. Patel, A. Miotello, M. Filippi, J. Mol. Catal. A: Chem. 298 (2009) 1–6.
[24] X.-L. Ding, X. Yuan, C. Jia, Z.-F. Ma, Int. J. Hydrogen Energy 35 (2010) 11077–11084.
[25] R. Fernandes, N. Patel, A. Miotello, Int. J. Hydrogen Energy 34 (2009) 2893–2900.
[26] H.-B. Dai, L.-L. Gao, Y. Liang, X.-D. Kang, P. Wang, J. Power Sources 195 (2010) 307–312.
[27] H.B. Dai, Y. Liang, P. Wang, X.D. Yao, T. Rufford, M. Lu, H.M. Cheng, Int. J. Hydrogen Energy 33 (2008) 4405–4412.
[28] J. Fang, X. Chen, B. Liu, S. Yan, M. Qiao, H. Li, H. He, K. Fan, Catal. J. 229 (2005) 97–104.
[29] J. Liang, Y. Li, Y. Huang, J. Yang, H. Tang, Z. Wei, P.K. Shen, Int. J. Hydrogen Energy 33 (2008) 4048–4054.
[30] C.-L. Hsueh, C.-Y. Chen, J.-R. Ku, S.-F. Tsai, Y.-Y. Hsu, F. Tsau, M.-S. Jeng, J. Power Sources 177 (2008) 485–492.
[31] R. Peña-Alonso, A. Sicurelli, E. Callone, G. Carturan, R. Raj, J. Power Sources 165 (2007) 315–323.
[32] N. Patel, R. Fernandes, G. Guella, A. Kale, A. Miotello, B. Patton, C. Zanchetta, J. Phys. Chem. C 112 (2008) 6968–6976.
[33] J. Delmas, L. Laversenne, I. Rougeaux, P. Capron, A. Garron, S. Bennici, D. Świerczyński, A. Auroux, Int. J. Hydrogen Energy 36 (2011) 2145–2153.
[34] R. López-Medina, J.L.G. Fierro, M.O. Guerrero-Pérez, M.A. Bañares, Appl. Catal. A: Gen. 375 (2010) 55–62.
[35] C.V. Rao, B. Viswanathan, Electrochim. Acta 55 (2010) 3002–3007.
[36] I. Alstrup, I. Chorkendorff, R. Candia, B.S. Clausen, H. Topsøe, J. Catal. 77 (1982) 397–409.
[37] A.B. Mandale, S. Badrinarayanan, S.K. Date, A.P.B. Sinha, J. Electron Spectrosc. Relat. Phenom. 33 (1984) 61–72.
[38] J.-M. Yan, X.-B. Zhang, H. Shioyama, Q. Xu, J. Power Sources 195 (2010) 1091–1094.
[39] B.S. Kwak, J. Kim, M. Kang, Int. J. Hydrogen Energy 35 (2010) 11829–11843.
[40] A. Galtayries, J. Grimblot, J. Electron Spectrosc. Relat. Phenom. 98–99 (1999) 267–275.
[41] A. Galtayries, S. Wisniewski, J. Grimblot, J. Electron Spectrosc. Relat. Phenom. 87 (1997) 31–44.
[42] G.-T. Kim, T.-K. Park, H. Chung, Y.-T. Kim, M.-H. Kwon, J.-G. Choi, Appl. Surf. Sci. 152 (1999) 35–43.
[43] M. Brun, A. Berthet, J.C. Bertolini, J. Electron Spectrosc. Relat. Phenom. 104 (1999) 55–60.
[44] X. Zhang, J. Zhao, F. Cheng, J. Liang, Z. Tao, J. Chen, Int. J. Hydrogen Energy 35 (2010) 8363–8369.
[45] J. Zhao, H. Ma, J. Chen, Int. J. Hydrogen Energy 32 (2007) 4711–4716.
[46] C.-H. Liu, B.-H. Chen, C.-L. Hsueh, J.-R. Ku, M.-S. Jeng, F. Tsau, Int. J. Hydrogen Energy 34 (2009) 2153–2163.
[47] M. Rakap, S. Özkar, Appl. Catal. B: Environ. 91 (2009) 21–29.
[48] P. Kukula, V. Gabova, K. Koprivova, P. Trtik, Catal. Today 121 (2007) 27–38.